

# User Guide for SWIFT v4 Wave Reconstruction

Alex Fisher  
September 29, 2023

## Overview

The methodology and codes described in this manual were developed to generate phase-resolved reconstructions of ocean waves over short time-space scales using SBG Ellipse measurements of wave motion collected by sparse arrays of Surface Wave Instrument Floats w/ Tracking (SWIFTs). Following initial exploration of the concept using SWIFT v4 (Thomson et al 2019) field data collected during the ONR Langmuir Circulation DRI, the methods described below have since been developed and tested using additional field and laboratory studies conducted as part of NSF OCE-1756040, NAVFAC Order N0002419F8709 T.D. #7101021 (WEC-UUV), and ARPA-E DIGITal Twin Model for Full-scale FLOATing Wind Turbines (DIGIFLOAT) projects.

This User Guide is intended as a quick reference guide to support future wave prediction efforts using the SWIFT v4 platform. The document is organized into the following sections: §1 Technical Approach, which provides a brief overview of the scientific approach described in full in Fisher et al (2021); §2 an overview of applications used in developing and testing the algorithm, including variations in methods employed; §3 a description of MATLAB codes used in wave reconstruction calculations; and §4 a description of the architecture available to enable real-time forecasting capability. All codes described herein have been used for research and development purposes; users should consider them *beta*-tested with no guarantee of performance.

## 1. Technical Approach

A brief overview of the mathematical approach used in SWIFT wave reconstructions is provided below, users are encouraged to refer to Fisher et al (2021) for a complete description of these methods. Following Connell et al (2015), the sea surface is formulated as the summation of plane waves to express a Gaussian wave field as a linear system of equations:

$$\eta_m = \exp(i(\mathbf{x}_m \cdot \mathbf{k}_n - \omega_n t_m - \phi_n)) \cdot A_n = \mathbf{P}\mathbf{A} \quad (1)$$

Where  $\eta$  is the measured surface displacement,  $\mathbf{P}$  is a  $M \times N$  propagator matrix that describes the translation of wave components in time and space, and  $\mathbf{A}$  is a  $N \times 1$  vector of unknown complex wave component amplitudes. When measurements of GPS horizontal velocities are available, (1) can be extended to a  $3M \times N$  matrix to aid in the decomposition of short-crested irregular waves in a straightforward manner, such that:

$$\begin{bmatrix} \eta_m \\ u_m \\ v_m \end{bmatrix} = \begin{bmatrix} \exp(i\phi)_{m,n} \\ \frac{k_x}{k} \exp(i\phi)_{m+M,n} \\ \frac{k_y}{k} \exp(i\phi)_{m+2M,n} \end{bmatrix} A_n \quad (2)$$

where  $\phi = \mathbf{x}_m \cdot \mathbf{k}_n - \omega_n t_m$  and  $\eta, u, v$ , indicate vertical displacement and horizontal velocities, respectively. If the linear system of equations shown is overdetermined (i.e.  $M > N$ ),  $M$  measurements of vertical displacement can be used to decompose the irregular free surface into  $N$  free wave components with Fourier amplitudes,  $A$ , using a least-squares approach. By inverting equation (1) or (2) and solving for  $A$ , a reduced-order approximation of the sea surface can be project time space and time to yield predictions of instantaneous wave conditions at a target location over a finite reconstruction horizon.

To avoid overfitting of the least squares solution to limited observations, a constrained least squares approach is used in which component amplitudes are bound by observed directional wave spectra and the system is solved using a trust-region reflective algorithm. To simplify the mathematical solution of the constrained least squares problem, the propagator matrix is transformed to represent the real part of (2) as the sum of sines and cosines via Euler's formula, increasing the number of unknowns from  $N$  to  $2N$ . The resulting bound-variable least-squares problem can be expressed as follows:

$$\min_x \frac{1}{2} \|\mathbf{P}\mathbf{A} - \mathbf{x}\|_2^2$$

where  $\mathbf{x}$  denotes the  $3M \times 1$  vector of observations shown on the l.h.s of (2) and is subject to  $-a \leq A \leq a$ , where  $a$  is a component-wise upper bound on the magnitude of unknown wave amplitudes. Note that sine–cosine pairs used to express each real wave component are bound by the same value of  $a$ .

Following the collection of a contemporaneous wave burst, the solution space is specified *a priori* based on the number of measurements available and the average observed directional wave spectrum estimated from the previous hour of available displacement and surface velocity data. The frequency range is limited to frequencies that satisfy  $S(\omega)/\max(S(\omega)) < 5\%$  (Desmars et al., 2020) and directional range is limited to  $DTp - \pi/2 < \theta < DTp + \pi/2$ , where  $S(\omega)$  is the scalar wave energy spectrum and  $DTp$  is the peak wave direction. The solution is limited to 40 logarithmically-spaced frequency components and 25 directional components. The upper bound for the magnitude of wave amplitudes ( $a$ ) was specified by interpolating component amplitudes provided by the observed directional wave spectrum to the solution space and normalizing to preserve variance.

### *SWIFT measurements*

The SWIFT v4 is built around a Sutron Xpert microprocessor and data logger. The Xpert has a 32-bit processor, supports SD memory, and has multiple serial and ethernet ports. The Xpert logs the raw measurements from the SWIFT sensor payload, and performs onboard processing of certain data products. Once per hour, these products are then transmitted over Iridium satellite communication to a server on land. The SBG Ellipse-N is a miniature, high-performance MEMS based inertial system with an industrial GNSS receiver. The Ellipse-N inertial motion unit (IMU) features three-axis gyroscopes, accelerometers, and magnetometers. It also runs a real-time Extended Kalman Filter (EKF) for data fusion of its IMU and GPS measurements. In combining the IMU and GPS data streams, the EKF uses the advantages of each measurement to produce a

better position and orientation solution than from either measurement alone. The most critical measurement of the SWIFTs for real-time wave prediction is the buoy vertical position, or heave. This is generally a difficult measurement because it requires two integrations of the inertial accelerometer signal, which leads to drift in the position. At the same time, the accuracy of the GPS measurements is much worse in the vertical direction than horizontal. To solve this problem, SBG has developed an advanced high-pass filter for estimating heave in real-time for marine purposes. The filter is designed to limit phase and gain errors in wave motions with periods shorter than 15 seconds.

#### *Pre-processing data for reconstruction algorithm*

Generally, SWIFT data output from `reprocess_SBG.m` can be fed directly into the prediction algorithm with little additional processing necessary to achieve results. When using horizontal velocities to solve for short-crested sea states, excessive noise at high frequencies can reduce prediction accuracy. Within the current version of these codes, 5Hz SBG Ellipse GPS horizontal velocities are filtered using a 4<sup>th</sup> order Butterworth low-pass filter with 0.5Hz cutoff to reduce noise prior to passing them to the prediction routine.

When working in fetch-limited conditions, default offshore settings within `SBGwaves.m` may artificially reduce wave energy due to the high-frequency cutoff used to prune spectral wave moments. It's recommended that the upper frequency cutoff of 0.5 Hz be increased to resolve high-frequency wave energy, which should be done with care to minimize bias stemming from resonant buoy motion ( $\sim 2$  Hz) .

#### *Prediction Algorithm Pseudo-Code*

1. Determine local UTC coordinates of buoys using raw GPS coordinates provided by either SBG Ellipse or Airmar.
2. Filter SBG GPS velocities, if available, using 4<sup>th</sup> order low-pass Butterworth filter with 0.5Hz cutoff.
3. Estimate average directional wave spectra from most recent wave burst using all available data from prediction buoy array.
4. Calculate mean wave period and peak wave direction to specify solution space and prediction interval.
5. Prescribe lead time used in reconstruction (e.g. how far into the future to forecast for a given location) using the distance from the nearest SWIFT to target location divided by the observed average wave period.
6. Initialize prediction variables:  $t_p$ ,  $\eta_p$ ,  $u_p$ ,  $v_p$
7. Subset SBG heave and velocity data into blocks of length  $9T_{m0}f_s$ , where  $f_s$  is the sampling frequency (5Hz), ensuring that subsetted SWIFT SBG measurements have raw timestamps that fall within the same period. See Section 4.2 in Fisher et al (2021) for a discussion of how the number of measurements influences prediction accuracy.
8. Pass each measurement block to reconstruction algorithm to predict sea surface elevation over short time interval (e.g.  $\sim 1$ s), advancing the prediction interval

smoothly to produce a rolling prediction of instantaneous sea surface elevations over each SWIFT burst.

### *Evaluating Prediction Accuracy*

To quantify the skill of the inverse model relative to spectral wave predictions, a mean-square-error skill score is defined as:

$$Skill\ Score = 1 - \frac{MSE_p}{MSE_s}$$

where  $MSE_p$  and  $MSE_s$  are the mean square errors between measured  $\eta(t)$  and predicted  $\tilde{\eta}(t)$  at the target location, for the inverse linear model and spectral wave model, respectively. Surface elevation time series used in  $MSE_s$  are generated from the summation of wave components with amplitudes drawn from a Rayleigh distribution described by the observed wave spectrum with randomized phase. In an ensemble sense,  $MSE_s$  is typically less (larger) than observed mean values of  $\eta^2$  when evaluated for wave envelope (surface displacement) time series.

## 2. Summary of Recent Applications & Known Issues

A summary of applications in which the reconstruction algorithm was used is shown in Table 1. Note that the spectral cutoff frequency and window size used in producing rolling predictions was adjusted based on the incident wave conditions. Horizontal GPS velocities were not used in the reconstruction for data collected in Lake Washington and Puget Sound tests due to low signal-to-noise ratios in small sea states. GPS positions were not available in the NSWC MASK Basin.

**Table 1: Summary of SWIFT wave reconstruction applications**

	<b>Sig. Wave Height [m]</b>	<b>Peak Period [s]</b>	<b>Spectral cutoff freq</b>	<b>Use GPS velocities</b>	<b>Rolling Window [s]</b>	<b>Skill Score</b>
<b>NE Pacific</b>	2.8 - 4.4	8.6 – 13.7	0.5 Hz	Yes	1	63%
<b>NE Atlantic</b>	1.0 – 3.9	4-15	0.5 Hz	Yes	1	67%
<b>Lk WA/Puget Sound</b>	0.1 - 0.4	1.5-2.75	2 Hz	No	0.6	~50%
<b>NSWC MASK Basin</b>	0.1-0.35	1.7 – 3.36	2 Hz	N/A	0.5	65%

### *Positional Uncertainty*

Drift in GPS positions can introduce substantial error for wave reconstructions in which dominant wavelengths are on the same order as positional uncertainty (e.g. short waves). An example is illustrated in Figure 1, taken from Puget Sound tests conducted in Winter 2023. In this example, artificial drift in the position of SWIFTs 24 and 25, which was similar to the average wavelength of the incident wave field, contributed to reduced reconstruction accuracy due to significant phase errors that propagated through the model inversion. A similar result was observed in the MASK basin tests, in which GPS positions were unavailable and burst-averaged buoy positions were estimated via trilateration using a handheld rangefinder.

### *Effective Prediction Zone*

The effective prediction zone for a least-squares solution is dependent on wave geometry and spectral bandwidth in short-crested seas, with a maximum forecast horizon between  $1-3T_{m0}$ . Due to the curve-fitting nature of the algorithm, versus a forward-solving dynamical model, the effective prediction zone generally constitutes a subspace of the theoretical prediction zone defined by Qi et al (2018). Observational and numerical results indicate that reconstructed wave fields are most accurate along the centerline of the prediction envelope and decay with increasing transverse distance.

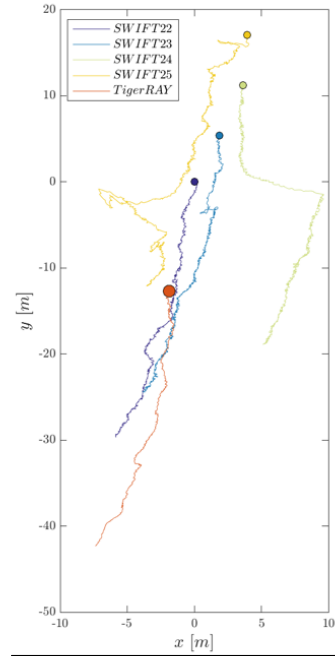


Figure 1: Example SWIFT drift tracks illustrating scale of positional uncertainty.

### 3. MATLAB codebase

**Table 2: MATLAB codes used in SWIFT wave reconstruction**

<b>batch_process_wave_predictions.m</b>	wrapper for run_LS_prediction_SWIFTS.m for batch generating predictions from multiple SWIFT bursts
<b>calculate_skillscores.m</b>	batch calculation of skill scores, wraps prediction_skill_score.m
<b>leastSquaresWavePropagation.m</b>	prediction algorithm engine
<b>pred_envelope_distributions.m</b>	Determine number of predictions for which the target location was enveloped in the theoretical prediction zone
<b>pred_enevelope.m</b>	Calculate theoretical prediction envelope based on geometric arguments in Qi et al (2018).
<b>prediction_skill_score.m</b>	Calculate Skill Score using measurements and synthetic realizations of spectral waves generated using the WAFO toolkit.
<b>reprocess_LS_predictions.m</b>	Use least-squares solutions to reconstruct sea surface in (x,y,t) space
<b>run_LS_prediction_SWIFTS.m</b>	Feeds SWIFT data into prediction algorithm
<b>sbg_positions.m</b>	Reprocess raw SBG data to store UTM (x,y) coordinates in SWIFT structure

### 4. Realtime forecasting architecture